

# AReLU: Attention-based Rectified Linear Unit

Dengsheng Chen

School of Computer

National University of Defense Technology

Kai Xu\*

School of Computer

National University of Defense Technology

## Abstract

Element-wise activation functions play a critical role in deep neural networks by affecting the expressivity power and the learning dynamics. Learning-based activation functions have recently gained increasing attention and success. We propose a new perspective of learnable activation function through formulating them with *element-wise attention mechanism*. In each network layer, we devise an attention module which learns an element-wise, sign-based attention map for the pre-activation feature map. The attention map scales an element based on its sign. Adding the attention module with a rectified linear unit (ReLU) results in an amplification of positive elements and a suppression of negative ones, both with learned, data-adaptive parameters. We coin the resulting activation function Attention-based Rectified Linear Unit (AReLU). The attention module essentially learns an element-wise residue of the activated part of the input, as ReLU can be viewed as an identity transformation. This makes the network training more resistant to gradient vanishing. The learned attentive activation leads to well-focused activation of relevant regions of a feature map. Through extensive evaluations, we show that AReLU significantly boosts the performance of most mainstream network architectures with only two extra learnable parameters per layer introduced. Notably, AReLU facilitates fast network training under small learning rates, which makes it especially suited in the case of transfer learning. Our source code has been released at: <https://github.com/densechen/AReLU>.

## 1 Introduction

Activation functions, introducing nonlinearities to artificial neural networks, is essential to networks' expressivity power and learning dynamics. Designing activation functions that facilitate fast training of accurate deep neural networks is an active area of research [23, 9, 35, 7, 13, 17, 2, 28]. Aside from the large body of hand-designed functions, learning-based approaches recently start to gain more attention and success [1, 11, 24, 25, 10]. The existing learnable activation functions are motivated either by relaxing/parameterizing a non-learnable activation function (e.g. Rectified Linear Units (ReLU) [26]) with learnable parameters [11], or by seeking for a data-driven combination of a pool of pre-defined activation functions [24]. Learning-based methods make activation functions data-adaptive through introducing degrees of freedom and/or enlarging the hypothesis space explored.

In this work, we propose a new perspective of learnable activation functions through formulating them with *element-wise attention mechanism*. A straightforward motivation of this is a plain observation that both activation functions and element-wise attention functions are applied as a network module with *element-wise multiplication*. More intriguingly, learning element-wise activation functions in a neural network can be intuitively viewed as task-oriented attention mechanism [6, 36], i.e., *learning where (which element in the input feature map) to attend (activate) given an end task*. This motivates the arguably more interpretable formulation of *attentive activation functions*.

Attention mechanism has been a cornerstone in deep learning. It directs the network to learn which part of the input is more relevant w.r.t. or contributes more to the output. There have been many variants of attention modules with plentiful successful applications. In natural language processing,

\*Corresponding author (kevin.kai.xu@gmail.com). Personal Homepage: [www.kevinkaixu.net](http://www.kevinkaixu.net).



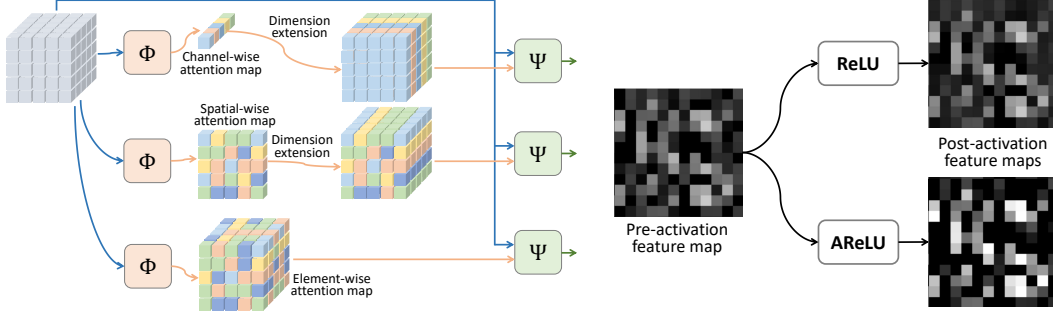


Figure 1: Left: An illustration of attention mechanisms with attention map at different granularities. Right: An visualization of pre-activation and post-activation feature maps obtained with ReLU and AReLU on a testing image of the handwritten digit dataset MNIST [20].

vector-wise attention is developed to model the long-range dependencies in a sequence of word vectors [21, 33]. Many computer vision tasks utilize pixel-wise or channel-wise attention modules for more expressive and invariant representation learning [36, 5]. Element-wise attention [3] is the most fine-grained where each element of a feature volume can receive different amount of attention. Consequently, it attains high expressivity with neuron-level degrees of freedom.

Inspired by that, we devise for each layer of a network an element-wise attention module which learns a sign-based attention map for the pre-activation feature map. The attention map scales an element based on its sign. Through adding the attention and a ReLU module, we obtain Attention-based Rectified Linear Unit (AReLU) which amplifies positive elements and suppresses negative ones, both with learned, data-adaptive parameters. The attention module essentially learns an element-wise residue for the activated elements with respect to the ReLU since the latter can be viewed as an identity transformation. This helps ameliorate the gradient vanishing issue effectively. Through extensive experiments on several public benchmarks, we show that AReLU significantly boosts the performance of most mainstream network architectures with only two extra learnable parameters per layer introduced. Moreover, AReLU enables fast learning under small learning rates, making it especially suited for transfer learning. We also demonstrate with feature map visualization that the learned attentive activation achieves well-focused, task-oriented activation of relevant regions.

## 2 Method

We start by describing attention mechanism and then introduce element-wise sign-based attention mechanism based on which AReLU is defined. The optimization of AReLU then follows.

### 2.1 Attention Mechanism

Let us denote  $V = \{v_i\} \in \mathbb{R}^{D_v^1 \times D_v^2 \times \dots}$  a tensor representing input a data or feature volume. Function  $\Phi$ , parameterized by  $\Theta = \{\theta_i\}$ , is used to compute an attention map  $S = \{s_i\} \in \mathbb{R}^{D_v^{\theta(1)} \times D_v^{\theta(2)} \times \dots}$  over a subspace of  $V$  (let  $\theta(\cdot)$  denote a correspondence function for the indices of dimension):

$$s_i = \Phi(v_i, \Theta).$$

$\Phi$  can be implemented by a neural network with  $\Theta$  being its learnable parameters.

We can modulate the input  $V$  with the attention map  $S$  using a function  $\Psi$ , obtaining the output  $U = \{u_i\} \in \mathbb{R}^{D_v^1 \times D_v^2 \times \dots}$ :

$$u_i = \Psi(v_i, s_i).$$

$\Psi$  is an element-wise multiplication. In order to perform element-wise multiplication, one needs to first extend  $S$  to the full dimension of  $V$ . We next review various attention mechanisms with attention map at different granularities. Figure 1(left) gives an illustration of various attention mechanisms.

**Vector-wise Attention Mechanism** In NLP, attention maps are usually computed over different word vectors. In this case,  $V = \{v_i\} \in \mathbb{R}^{N \times D}$  represents a sequence of  $N$  feature vectors with dimension  $D$ .  $S = \{s_i\} \in \mathbb{R}^N$  is a sequence of attention values for the corresponding vectors.



**Channel-wise Attention Mechanism** In computer vision, a feature volume  $V = \{v_i\} \in \mathbb{R}^{W \times H \times C}$  has a spatial dimension of  $W \times H$  and a channel dimension of  $C$ .  $S = \{s_i\} \in \mathbb{R}^C$  is an attention map over the  $C$  channels. All elements in each channel share the same attention value.

**Spatial-wise Attention Mechanism** Considering again  $V = \{v_i\} \in \mathbb{R}^{W \times H \times C}$  with a spatial dimension of  $W \times H$ .  $S = \{s_i\} \in \mathbb{R}^{W \times H}$  is an attention map over the spatial dimension. All channels of a given spatial location share the same attention value.

**Element-wise Attention Mechanism** Given a feature volume  $V = \{v_i\} \in \mathbb{R}^{W \times H \times C}$  containing  $W \times H \times C$  elements, we compute an attention map over the whole volume (all elements), i.e.,  $S = \{s_i\} \in \mathbb{R}^{W \times H \times C}$ , so that each element has an independent attention value.

## 2.2 ELement-wise Sign-based Attention (ELSA)

We propose, ELSA, a new kind of element-wise attention mechanism which is used to define our attention-based activation. Considering a feature volume  $V = \{v_i\} \in \mathbb{R}^{W \times H \times C}$ , we compute an element-wise attention map  $S = \{s_i\} \in \mathbb{R}^{W \times H \times C}$ :

$$s_i = \Phi(v_i, \Theta) = \begin{cases} C(\alpha), & v_i < 0 \\ \sigma(\beta), & v_i \geq 0 \end{cases}$$

where  $\Theta = \{\alpha, \beta\} \in \mathbb{R}^2$  is learnable parameters.  $C(\cdot)$  clamps the input variable into  $[0.01, 0.99]$ .  $\sigma$  is the sigmoid function. The modulation function  $\Psi$  is defined as:

$$u_i = \Psi(v_i, s_i) = s_i v_i.$$

In ELSA, positive and negative elements receive different amount of attention determined by the two parameters  $\alpha$  and  $\beta$ , respectively. Therefore, it can also be regarded as sign-wise attention mechanism. With only two learnable parameters, ELSA is light-weight and easy to learn.

## 2.3 AReLU: Attention-based Rectified Linear Units

We represent the function  $\Phi$  in ELSA with a network layer with learnable parameters  $\alpha$  and  $\beta$ :

$$\mathcal{L}(x_i, \alpha, \beta) = \begin{cases} C(\alpha)x_i, & x_i < 0 \\ \sigma(\beta)x_i, & x_i \geq 0 \end{cases}$$

where  $X = \{x_i\}$  is the input of the current layer. In constructing an activation function with ELSA, we combine it with the standard Rectified Linear Units

$$\mathcal{R}(x_i) = \begin{cases} 0, & x_i < 0 \\ x_i, & x_i \geq 0 \end{cases}$$

Adding them together leads to a learnable activation function:

$$\mathcal{F}(x_i, \alpha, \beta) = \mathcal{R}(x_i) + \mathcal{L}(x_i, \alpha, \beta) = \begin{cases} C(\alpha)x_i, & x_i < 0 \\ (1 + \sigma(\beta))x_i, & x_i \geq 0 \end{cases}$$

This combination amplifies positive elements and suppresses negative ones based on the learned scaling parameters  $\beta$  and  $\alpha$ , respectively. Thus, ELSA learns an element-wise residue for the activated elements w.r.t. ReLU which is an identity transformation, which helps ameliorate gradient vanishing.

## 2.4 The Optimization of AReLU

AReLU can be trained using back-propagation jointly with all other network layers. The update formulation of  $\alpha$  and  $\beta$  can be derived with the chain rule. Specifically, the gradient of  $\alpha$  is:

$$\frac{\partial \mathcal{E}}{\partial \alpha} = \frac{\partial \mathcal{E}}{\partial \mathcal{F}(x_i, \alpha, \beta)} \frac{\partial \mathcal{F}(x_i, \alpha, \beta)}{\partial \alpha}$$

where  $\mathcal{E}$  is the error function to be minimized. The term  $\frac{\partial \mathcal{E}}{\partial \mathcal{F}(x_i, \alpha, \beta)}$  is the gradient propagated from the deeper layer. The gradient of the activation of  $X$  with respect to  $\alpha$  is given by:

$$\frac{\partial \mathcal{F}(X, \alpha, \beta)}{\partial \alpha} = \sum_{x_i < 0} x_i$$



Here, the derivative of the clamp function  $C(\cdot)$  is handled simply by detaching the gradient back-propagation when  $\alpha < 0.01$  or  $\alpha > 0.99$ .

The gradient of the activation of  $X$  with respect to  $\beta$  is:

$$\frac{\partial \mathcal{F}(X, \alpha, \beta)}{\partial \beta} = \sum_{x_i \geq 0} \sigma(\beta)(1 - \sigma(\beta))x_i$$

The gradient of the activation with respect to input  $x_i$  by:

$$\frac{\partial \mathcal{F}(x_i, \alpha, \beta)}{\partial x_i} = \begin{cases} \alpha, & x_i < 0 \\ 1 + \sigma(\beta), & x_i \geq 0 \end{cases}$$

It can be found that AReLU amplifies the gradients propagated from the downstream when the input is activated since  $1 + \sigma(\beta) > 1$ ; it suppresses the gradients otherwise. On the contrary, there is no such amplification effect in the standard ReLU and its variants (e.g., PReLU [11]) — only suppression is available. The ability to amplify the gradients over the activated input helps avoiding gradient vanishing, and thus speeds up the training convergence of the model (see Figure 3). Moreover, the amplification factor is learned to dynamically adapt to the input and is confined with the sigmoid function. This makes the activation more data-adaptive and stable (see Figure 1(right) for a visual comparison of post-activation feature maps by AReLU and ReLU). The suppression part is similar to PReLU which learns the suppression factor for ameliorating zero gradients.

AReLU introduces a very small number of extra parameters which is  $2L$  for an  $L$ -layer network. The computational complexity due to AReLU is negligible for both forward and backward propagation.

Note that the gradients of  $\alpha$  and  $\beta$  depend on the entire feature volume  $X$ . This means that ELISA can be regarded as a global attention mechanism: Although the attention map is computed in an element-wise manner, the parameters are learned globally accounting for the impact of the full feature volume. This makes our AReLU more data-adaptive and hence the whole network more expressive.

We adopt the momentum method for updating  $\alpha$  and  $\beta$ :

$$\Delta\alpha := \mu\Delta\alpha + \epsilon\frac{\partial\mathcal{E}}{\partial\alpha}, \quad \Delta\beta := \mu\Delta\beta + \epsilon\frac{\partial\mathcal{E}}{\partial\beta},$$

where  $\mu$  is the momentum and  $\epsilon$  the learning rate. It is worth noticing that a weight decay ( $L_2$  regularization) tends to push  $\alpha$  to zero. Confining  $\alpha$  within  $[0.01, 0.99]$  mitigates this issue.

### 3 Experiments

We first study the robustness of AReLU in terms of parameter initialization. We then conduct comprehensive evaluation with three standard classification benchmarks (MNIST [20], CIFAR10 and CIFAR100 [19]) and one image segmentation benchmark. We compare AReLU with 18 different activation functions including 13 non-learnable ones and 5 learnable ones; see the list in Table 1. The number of learnable parameters for each learnable activation function are also given in the table.

#### 3.1 Initialization of Learnable Parameter $\alpha$ and $\beta$

For evaluation purpose, we design a neural network (MNIST-Conv) with three convolutional layers each followed by a max-pooling layer and an AReLU, and finally a fully connected layer followed by a softmax layer. *Details of this network can be found in the supplemental material.* The experiment on parameter initialization is conducted with MNIST-Conv over the MNIST dataset. As shown in Figure 2(a), AReLU is insensitive to the initialization of  $\alpha$  and  $\beta$ . Different initial values result in close convergence rate and classification accuracy. Generally, a large initial value of  $\beta$  can speed up the convergence. Figure 2(b) shows the learning procedure of the two parameters and (c) plots the learned final AReLU's for the three convolutional layers. In the following experiments, we initialize  $\alpha = 0.9$  and  $\beta = 2.0$  for the MNIST dataset since it is easy to achieve a high accuracy for this dataset and hence convergence speed is more of a concern. In addition, we initialize  $\alpha = 0.75$  and  $\beta = 1.0$  for the CIFAR and the brain image dataset to attain a higher accuracy.



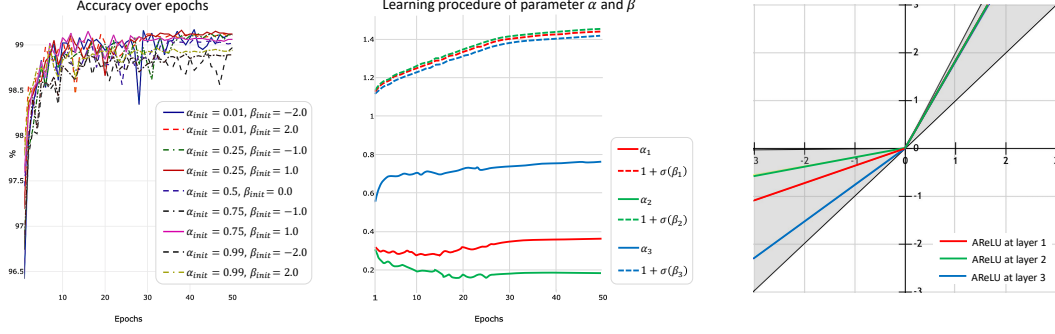


Figure 2: (a): Plot of accuracy over epochs for networks trained with different initialization of  $\alpha$  and  $\beta$ . A larger initial  $\beta$  leads to faster convergence and higher accuracy is obtained when  $\alpha$  is initialized to 0.25 or 0.75. (b): The learning procedure of  $\alpha$  and  $\beta$  which are initialized to 0.25 and 1.0, respectively. (c): The learned final AReLU's for the three convolutional layers of the MNIST-Conv network. The shaded region gives the range of AReLU curves.

### 3.2 Performance on MNIST

On the MNIST dataset, we evaluate MNIST-Conv implemented with different activation functions and trained with the ADAM or SGD optimizer. The activation function is placed after each max-pooling layers. We compare AReLU with both learnable and non-learnable activation functions under different learning rates of  $1 \times 10^{-2}$ ,  $1 \times 10^{-3}$ ,  $1 \times 10^{-4}$ , and  $1 \times 10^{-5}$ . To compare the convergence speed of different activation functions, we report the accuracy after the first epoch, again taking the mean over five times training; see Table 1. In the table, we report the improvement of AReLU over the best among other non-learnable and learnable methods. In Figure 3, we plot the mean accuracy over increasing number of training epochs.

As shown in Table 1, AReLU outperforms most existing non-learnable and learnable activation functions in terms of convergence speed and final classification accuracy on MNIST. A note-worthy phenomenon is that AReLU can achieve a more effective training with a small learning rate (see the significant improvement when the learning rate is  $1 \times 10^{-4}$  or  $1 \times 10^{-5}$ ) than the alternatives. This can also be observed from Figure 3. Generally, smaller learning rates would cause lower learning efficiency since the vanishing gradient issue is intensified in such case. AReLU can overcome this difficulty thanks to its gradient amplification effect. Efficient learning with a small learning rate is very useful in transfer learning where a pre-trained model is usually fine-tuned on a new domain/dataset with a small learning rate, while it is difficult to most existing deep networks. In the next experiment, we demonstrate how AReLU improves learning efficiency in transfer learning.

### 3.3 Performance in Transfer Learning

We evaluate transfer learning of MNIST-Conv with different activation functions between two datasets: MNIST and SVHN<sup>2</sup>. The data preprocessing for adapting the two datasets follows [31]. We train three models and test them on SVHN: 1) one is trained directly on SVHN without any pretraining, 2) one trained on MNIST but not finetuned on SVHN, and 3) one pretrained on MNIST and finetuned on SVHN. In pretraining, we train MNIST-Conv using SGD with a learning rate of 0.01 for 20 epochs which is sufficient for all model variants to converge. In finetuning, we train the model on SVHN with a learning rate of  $1 \times 10^{-5}$ , using SGD optimizer for 100 epochs.

The testing results on SVHN are partially reported in Table 2; *see the full table in the supplemental material*. Without pretraining, it is hard to obtain a good accuracy on SVHN for all models, among which AReLU performs the best. In transfer learning (pretrain + finetune), AReLU outperforms all other activation functions, thanks to its high learning efficiency with small learning rates.

### 3.4 Performance on CIFAR10

In this experiment, we compare all the activation functions with three widely used network architectures on the CIFAR10 dataset. The three networks are VGG-11 [32], ResNet-18 [12], and

<sup>2</sup><http://ufldl.stanford.edu/housenumbers/>



Table 1: Mean testing accuracy (%) on MNIST for five trainings of MNIST-Conv after the *first epoch* with different optimizers and learning rates. We compare AReLU with 13 non-learnable and 5 learnable activation functions. The number of parameters per activation unit are listed beside the name of the learnable activation functions. The best numbers are shown in bold text with blue color for non-learnable methods and red for learnable ones. At the bottom of the table, we report the improvement of AReLU over the best among other non-learnable and learnable methods, in blue and red color respectively.

Learning Rate	$1 \times 10^{-2}$		$1 \times 10^{-3}$		$1 \times 10^{-4}$		$1 \times 10^{-5}$	
Optimizer	Adam	SGD	Adam	SGD	Adam	SGD	Adam	SGD
CELU [2]	97.76	96.12	96.21	62.81	84.01	13.07	24.84	9.60
ELU [7]	97.82	96.17	96.22	58.10	<b>85.67</b>	14.07	19.77	10.13
GELU [13]	<b>98.49</b>	94.90	95.79	12.55	83.72	11.49	15.20	<b>10.92</b>
LeakyReLU [23]	97.80	95.59	95.86	35.90	84.08	10.28	15.41	10.73
Maxout [9]	97.04	95.81	96.14	71.75	84.81	10.79	18.83	9.06
ReLU [26]	97.75	95.02	95.40	36.01	84.02	10.68	15.25	8.73
ReLU6 [18]	97.77	95.32	96.09	43.42	81.39	10.23	14.33	9.56
RReLU [35]	98.09	95.88	95.65	53.33	84.51	9.57	16.53	10.28
SELU [17]	97.25	<b>96.52</b>	<b>96.61</b>	<b>82.36</b>	85.36	<b>16.49</b>	<b>30.04</b>	9.59
Sigmoid	47.16	11.04	83.59	11.35	11.37	9.92	10.52	10.10
Softplus [8]	96.38	90.90	93.83	11.14	51.83	9.19	10.21	9.89
Swish [28]	98.10	94.02	95.91	11.44	83.91	10.69	11.39	9.47
Tanh	96.93	94.22	96.45	57.70	79.25	11.73	27.05	10.31
APL [1] (2)	97.00	95.71	94.67	17.81	76.73	9.39	13.28	11.83
Comb [24] (1)	<b>98.28</b>	95.97	95.79	35.95	83.91	10.59	20.22	10.18
PAU [25] (10)	98.17	<b>97.67</b>	96.73	40.11	87.08	10.54	14.49	11.11
PReLU [11] (1)	98.22	95.72	95.87	45.73	85.81	12.08	14.51	9.88
SLAF [10] (2)	96.30	97.07	95.32	83.35	72.67	14.12	10.04	11.32
AReLU (2)	98.00	97.30	<b>97.13</b>	<b>93.13</b>	<b>90.44</b>	<b>47.78</b>	<b>38.39</b>	<b>14.25</b>
Improvement	-0.49	+0.78	+0.52	+10.77	+4.77	+31.29	+8.35	+3.33
Improvement	-0.28	-0.37	+0.40	+9.78	+3.36	+33.66	+18.17	+2.42

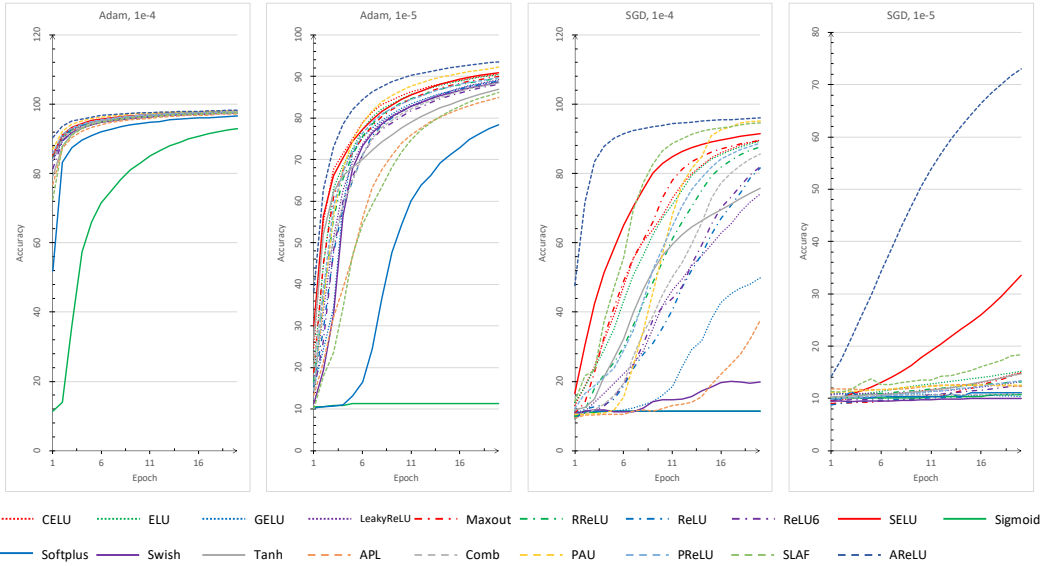


Figure 3: The plots of mean testing accuracy (%) on MNIST for five-time trainings of MNIST-Conv over increasing training epochs with different optimizers and learning rates. AReLU attains a faster training for both optimizers when the learning rate is set to  $1 \times 10^{-4}$  or  $1 \times 10^{-5}$ .



Table 2: Test accuracy (%) on SVHN by models (with different activation functions) trained directly on SVHN (w/o pretrain), trained on MNIST but not finetuned (w/o finetune), as well as pretrained on MNIST and finetuned on SVHN (pretrain+finetune). *See full table in the supplemental material.*

	ELU	GELU	Maxout	ReLU	SELU	Softplus	APL	Comb	PAU	PReLU	SLAF	AReLU
w/o pretrain	19.59	19.59	23.01	19.58	19.58	19.58	19.58	19.58	19.58	19.58	19.58	<b>24.95</b>
w/o finetune	31.95	<b>37.38</b>	36.52	36.87	32.57	14.39	36.20	35.89	24.67	33.45	35.74	31.91
pretrain+finetune	72.39	71.64	71.88	70.58	73.43	69.18	74.21	69.92	74.70	71.15	73.12	<b>76.77</b>

Table 3: Test accuracy of five times training on CIFAR10.

Network	VGG-11 [32]		ResNet-18 [12]		MobileNet [15]	
Accuracy (%)	best	mean	best	mean	best	mean
CELU [2]	89.76	89.92	92.02	91.87	90.07	89.91
ELU [7]	90.10	89.92	91.85	91.70	90.09	89.80
GELU [13]	91.54	91.29	94.29	94.18	<b>92.56</b>	<b>92.74</b>
LeakyReLU [23]	<b>91.89</b>	<b>91.75</b>	<b>94.78</b>	<b>94.65</b>	90.75	90.65
Maxout [9]	88.42	88.22	—	—	—	—
RReLU [35]	91.52	91.38	94.10	94.05	92.48	92.20
ReLU [26]	91.70	91.57	94.36	94.32	90.67	90.52
ReLU6 [18]	91.73	91.48	94.74	94.59	90.69	90.60
SELU [17]	89.48	89.18	91.61	91.38	88.61	88.56
Sigmoid	—	—	81.11	80.49	79.37	77.78
Softplus[8]	86.94	86.51	88.97	88.56	87.45	87.10
Swish [28]	90.84	90.75	93.67	93.57	91.94	91.74
Tanh	90.22	89.99	91.61	91.50	88.74	88.54
APL [1] (2)	91.65	91.03	94.60	93.79	90.88	90.07
Comb [24] (1)	90.90	63.32	93.82	93.28	92.04	91.51
PAU [25] (10)	91.76	90.94	<b>94.78</b>	<b>94.52</b>	<b>92.71</b>	<b>92.12</b>
PReLU [11] (1)	91.13	90.11	93.82	93.61	91.71	91.16
SLAF [10] (2)	—	—	—	—	—	—
AReLU (2)	<b>91.90</b>	<b>91.59</b>	<b>94.78</b>	94.43	91.68	91.56
Improvement	+0.01	−0.16	+0.00	−0.22	−0.88	−1.18
Improvement	+0.20	+0.56	+0.00	−0.09	−1.03	−0.56

MobileNet [15]. We use the same training configuration for all the three networks. The initial learning rate is set to 0.1 and is multiplied by 0.1 at the 50-th and 75-th epochs. We train for 100 epochs with the batch size being 128, the weight decay being  $5 \times 10^{-4}$ , and the Nesterov momentum being 0.9.

For each network with each activation function, we train five times and report both the mean and the best test accuracy in Table 3. From the comparison, ARReLU performs the best with VGG-11, and reasonably well with ResNet-18 and MobileNet, with only two learnable parameters. ARReLU outperforms the other learnable activation functions with comparable number of learnable parameters. ARReLU works comparably well against PAU [25] although the latter contains five times learnable parameters. In conclusion, ARReLU adapts well to different network architectures.

### 3.5 Performance on CIFAR100

We evaluate the performance of ARReLU with six mainstream networks on CIFAR100. We follow the training configuration in [27]: The learning rate is initialized as 0.1 and multiplied by 0.2 at the 60-th, 120-th, and 160-th epochs. The networks are trained for 200 epochs with the batch size being 64, the weight decay being  $5 \times 10^{-4}$ , and the Nesterov momentum being 0.9.

For each network with each activation function, we run five times of training and report the mean accuracy in top-1 and top-5 classification results; see Table 4. By introducing attention mechanism to the vanilla ReLU, all the six networks obtain performance boosting.

We also conduct a qualitative analysis of ARReLU by visualizing the learned feature maps using Grad-CAM [30] using testing images of CIFAR100. Grad-CAM is a recently proposed network visualization method which utilizes gradients to depict the importance of the spatial locations in a feature map. Since gradients are computed with respect to a specific image class, Grad-CAM visualization can be regarded as a task-oriented attention map.



Table 4: Mean test accuracy in top-1 and top-5 results of five times training on CIFAR100.

Accuracy (%)	@top-1	@top-5	@top-1	@top-5	@top-1	@top-5
Network	VGG-11 [32]		VGG-13 [32]		SEResNet18 [34]	
ReLU	68.03	87.49	71.92	90.05	76.80	93.16
AReLU	<b>68.04</b>	<b>88.27</b>	<b>71.93</b>	<b>90.86</b>	<b>76.94</b>	<b>93.66</b>
Improvement	+0.01	+0.78	+0.01	+0.81	+0.14	+0.50
Network	ResNet-18 [12]		ShuffleNet-v2 [22]		SqueezeNet [16]	
ReLU	76.35	93.18	68.56	90.92	69.96	91.29
AReLU	<b>76.40</b>	<b>93.39</b>	<b>69.63</b>	<b>91.37</b>	<b>70.19</b>	<b>91.41</b>
Improvement	+0.05	+0.20	+1.07	+0.45	+0.23	+0.12

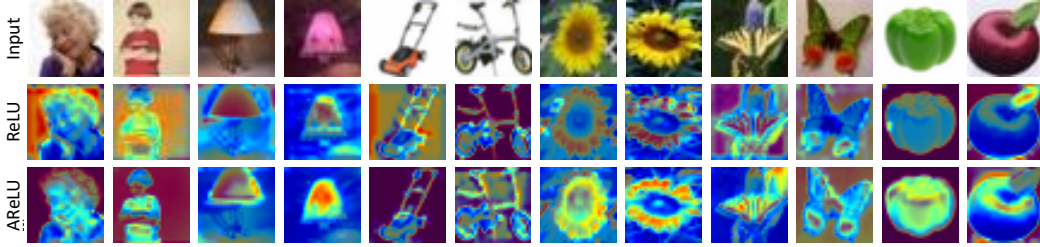


Figure 4: Grad-CAM visualization of feature maps extracted by ResNet-18 with AReLU and ReLU. The first row is the testing images of CIFAR100.

In Figure 4, we visualize the first-layer feature map of ResNet-18. As shown in the figure, the feature maps learned with AReLU leads to semantically more meaningful activation of regions with respect to the target class. This is due to the data-adaptive, attentive ability of AReLU.

### 3.6 Performance in Image Segmentation

We test AReLU with UNet [29] for brain image segmentation. We use the Kaggle Brain MRI Segmentation dataset<sup>3</sup> and follow the implementation details in [4]. The dataset contains MRI from the TCIA LGG collection<sup>4</sup> with expert-approved segmentation masks. Figure 5 shows that AReLU leads to a faster training than ReLU and achieves a better segmentation accuracy (91.14% vs. 90.77% for the DSC metric [29]). *Extended results can be found in the supplemental material.*

## 4 Conclusion

We have presented AReLU, a new learnable activation function formulated with element-wise sign-based attention mechanism. Networks implemented with AReLU can better mitigate the gradient vanishing issue and converge faster with small learning rates. This makes it especially useful in transfer learning where a pretrained model needs to be finetuned in the target domain with a small learning rate. AReLU can significantly boost the performance of most mainstream network architectures with only two extra learnable parameters per layer introduced. In the future, we would like to investigate the application/extension of AReLU to more diverse tasks such as object detection, language translation and even structural feature learning with graph neural networks.

## References

- [1] Forest Agostinelli, Matthew Hoffman, Peter Sadowski, and Pierre Baldi. Learning activation functions to improve deep neural networks. *arXiv preprint arXiv:1412.6830*, 2014.
- [2] Jonathan T Barron. Continuously differentiable exponential linear units. *arXiv preprint arXiv:1704.07483*, 2017.
- [3] Alexey Bochkovskiy, Chien-Yao Wang, and Hong-Yuan Mark Liao. Yolov4: Optimal speed and accuracy of object detection. *arXiv preprint arXiv:2004.10934*, 2020.

<sup>3</sup><https://www.kaggle.com/mateuszbuda/lgg-mri-segmentation>

<sup>4</sup><https://wiki.cancerimagingarchive.net/display/Public/TCGA-LGG>



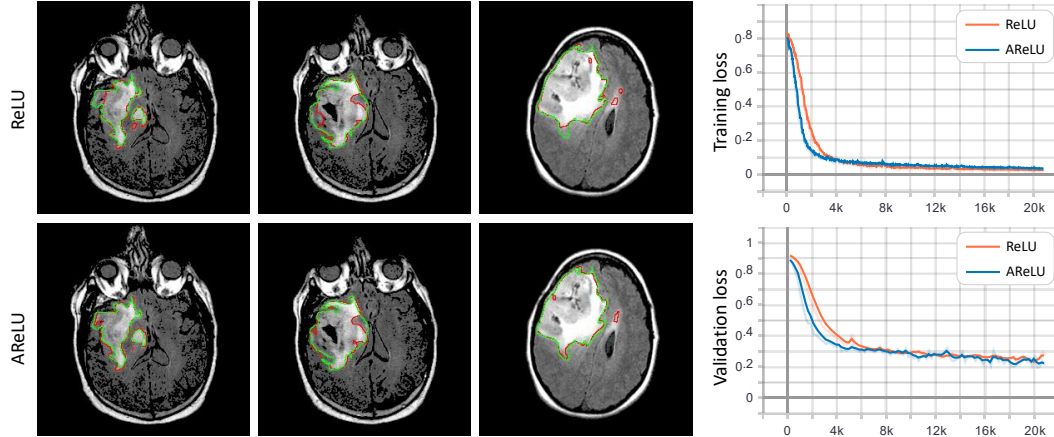


Figure 5: Left: Segmentation results of UNet with ReLU (top row) and AReLU (bottom). Prediction is depicted in red and ground-truth in green. Right: Training and validation loss over iterations.

- [4] Mateusz Buda, Ashirbani Saha, and Maciej A Mazurowski. Association of genomic subtypes of lower-grade gliomas with shape features automatically extracted by a deep learning algorithm. *Computers in biology and medicine*, 109:218–225, 2019.
- [5] Long Chen, Hanwang Zhang, Jun Xiao, Liqiang Nie, Jian Shao, Wei Liu, and Tat-Seng Chua. SCA-CNN: Spatial and channel-wise attention in convolutional networks for image captioning. In *Proceedings of the IEEE conference on computer vision and pattern recognition*, pages 5659–5667, 2017.
- [6] Jan K Chorowski, Dzmitry Bahdanau, Dmitriy Serdyuk, Kyunghyun Cho, and Yoshua Bengio. Attention-based models for speech recognition. In *Advances in neural information processing systems*, pages 577–585, 2015.
- [7] Djork-Arné Clevert, Thomas Unterthiner, and Sepp Hochreiter. Fast and accurate deep network learning by exponential linear units (elus). *arXiv preprint arXiv:1511.07289*, 2015.
- [8] Xavier Glorot, Antoine Bordes, and Yoshua Bengio. Deep sparse rectifier neural networks. In *Proceedings of the fourteenth international conference on artificial intelligence and statistics*, pages 315–323, 2011.
- [9] Ian J Goodfellow, David Warde-Farley, Mehdi Mirza, Aaron Courville, and Yoshua Bengio. Maxout networks. *arXiv preprint arXiv:1302.4389*, 2013.
- [10] Mohit Goyal, Rajan Goyal, and Brejesh Lall. Learning activation functions: A new paradigm for understanding neural networks, 2019.
- [11] Kaiming He, Xiangyu Zhang, Shaoqing Ren, and Jian Sun. Delving deep into rectifiers: Surpassing human-level performance on imagenet classification. In *Proceedings of the IEEE international conference on computer vision*, pages 1026–1034, 2015.
- [12] Kaiming He, Xiangyu Zhang, Shaoqing Ren, and Jian Sun. Deep residual learning for image recognition. In *Proceedings of the IEEE conference on computer vision and pattern recognition*, pages 770–778, 2016.
- [13] Dan Hendrycks and Kevin Gimpel. Gaussian error linear units (gelus). *arXiv preprint arXiv:1606.08415*, 2016.
- [14] Dan Hendrycks and Kevin Gimpel. Gaussian error linear units (gelus), 2016.
- [15] Andrew G Howard, Menglong Zhu, Bo Chen, Dmitry Kalenichenko, Weijun Wang, Tobias Weyand, Marco Andreetto, and Hartwig Adam. Mobilenets: Efficient convolutional neural networks for mobile vision applications. *arXiv preprint arXiv:1704.04861*, 2017.
- [16] Forrest N Iandola, Song Han, Matthew W Moskewicz, Khalid Ashraf, William J Dally, and Kurt Keutzer. Squeezenet: Alexnet-level accuracy with 50x fewer parameters and < 0.5 mb model size. *arXiv preprint arXiv:1602.07360*, 2016.
- [17] Günter Klambauer, Thomas Unterthiner, Andreas Mayr, and Sepp Hochreiter. Self-normalizing neural networks. In *Advances in neural information processing systems*, pages 971–980, 2017.



- [18] Alex Krizhevsky and Geoff Hinton. Convolutional deep belief networks on cifar-10. *Unpublished manuscript*, 40(7):1–9, 2010.
- [19] Alex Krizhevsky, Geoffrey Hinton, et al. Learning multiple layers of features from tiny images. 2009.
- [20] Yann LeCun, Léon Bottou, Yoshua Bengio, and Patrick Haffner. Gradient-based learning applied to document recognition. *Proceedings of the IEEE*, 86(11):2278–2324, 1998.
- [21] Minh-Thang Luong, Hieu Pham, and Christopher D Manning. Effective approaches to attention-based neural machine translation. *arXiv preprint arXiv:1508.04025*, 2015.
- [22] Ningning Ma, Xiangyu Zhang, Hai-Tao Zheng, and Jian Sun. Shufflenet v2: Practical guidelines for efficient cnn architecture design. In *Proceedings of the European Conference on Computer Vision (ECCV)*, pages 116–131, 2018.
- [23] Andrew L Maas, Awni Y Hannun, and Andrew Y Ng. Rectifier nonlinearities improve neural network acoustic models. In *Proc. icml*, volume 30, page 3, 2013.
- [24] Franco Manessi and Alessandro Rozza. Learning combinations of activation functions. In *2018 24th International Conference on Pattern Recognition (ICPR)*, pages 61–66. IEEE, 2018.
- [25] Alejandro Molina, Patrick Schramowski, and Kristian Kersting. Pad\`e activation units: End-to-end learning of flexible activation functions in deep networks. *arXiv preprint arXiv:1907.06732*, 2019.
- [26] Vinod Nair and Geoffrey E Hinton. Rectified linear units improve restricted boltzmann machines. In *Proceedings of the 27th international conference on machine learning (ICML-10)*, pages 807–814, 2010.
- [27] Gabriel Pereyra, George Tucker, Jan Chorowski, Łukasz Kaiser, and Geoffrey Hinton. Regularizing neural networks by penalizing confident output distributions. *arXiv preprint arXiv:1701.06548*, 2017.
- [28] Prajit Ramachandran, Barret Zoph, and Quoc V Le. Searching for activation functions. *arXiv preprint arXiv:1710.05941*, 2017.
- [29] Olaf Ronneberger, Philipp Fischer, and Thomas Brox. U-net: Convolutional networks for biomedical image segmentation. In *International Conference on Medical image computing and computer-assisted intervention*, pages 234–241. Springer, 2015.
- [30] Ramprasaath R Selvaraju, Michael Cogswell, Abhishek Das, Ramakrishna Vedantam, Devi Parikh, and Dhruv Batra. Grad-cam: Visual explanations from deep networks via gradient-based localization. In *Proceedings of the IEEE international conference on computer vision*, pages 618–626, 2017.
- [31] Hanul Shin, Jung Kwon Lee, Jaehong Kim, and Jiwon Kim. Continual learning with deep generative replay. In *Advances in Neural Information Processing Systems*, pages 2990–2999, 2017.
- [32] Karen Simonyan and Andrew Zisserman. Very deep convolutional networks for large-scale image recognition. *arXiv preprint arXiv:1409.1556*, 2014.
- [33] Ashish Vaswani, Noam Shazeer, Niki Parmar, Jakob Uszkoreit, Llion Jones, Aidan N Gomez, Łukasz Kaiser, and Illia Polosukhin. Attention is all you need. In *Advances in neural information processing systems*, pages 5998–6008, 2017.
- [34] Saining Xie, Ross Girshick, Piotr Dollár, Zhuowen Tu, and Kaiming He. Aggregated residual transformations for deep neural networks. In *Proceedings of the IEEE conference on computer vision and pattern recognition*, pages 1492–1500, 2017.
- [35] Bing Xu, Naiyan Wang, Tianqi Chen, and Mu Li. Empirical evaluation of rectified activations in convolutional network. *arXiv preprint arXiv:1505.00853*, 2015.
- [36] Kelvin Xu, Jimmy Ba, Ryan Kiros, Kyunghyun Cho, Aaron Courville, Ruslan Salakhudinov, Rich Zemel, and Yoshua Bengio. Show, attend and tell: Neural image caption generation with visual attention. In *International conference on machine learning*, pages 2048–2057, 2015.



# Appendices

## A Details of ConvMNIST

ConvMNIST is a VGG [32]-like network but with fewer layers, as shown in Figure 6. The activation layers will be placed with specified activation functions while experiments.

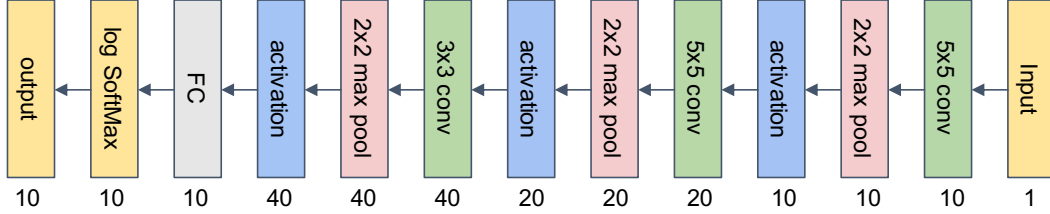


Figure 6: The network architecture of ConvMNIST. The number under the block indicates that output channels of current layer.

## B More results on MNIST

Table 5 reports the best testing accuracy on MNIST for five trainings of MNIST-Conv after the *first epoch* with different optimizers and learning rates. Table 7 shows mean testing accuracy of five-time training of MNIST-Conv trained for 20 epochs with different learning rates on MNIST. In Table 6, the best testing accuracy of five-time training of MNIST-Conv trained for 20 epochs with different learning rates on MNIST are reported. We compare AReLU with 13 non-learnable and 5 learnable activation functions. The number of parameters per activation unit are listed beside the name of the learnable activation functions. The best numbers are shown in bold text with blue color for non-learnable methods and red for learnable ones. At the bottom of the table, we report the improvement of AReLU over the best among other non-learnable and learnable methods, in blue and red respectively.

We also plot the mean training loss and testing accuracy of five runs with different optimizers and learning rates in Figure 7 and Figure 8.

## C Full result of transfer learning

The full table of transfer learning is shown in Table 8.

## D More results on Segmentation

We visualize the learning procedure (segmentation results) of UNet [29] on a testing MRI image over increasing number of learning iterations in Figure 9. AReLU leads to better segmentation than ReLU.



Table 5: Best testing accuracy (%) on MNIST for five trainings of MNIST-Conv after the *first epoch* with different optimizers and learning rates. We compare AReLU with 13 non-learnable and 5 learnable activation functions. The number of parameters per activation unit are listed beside the name of the learnable activation functions. The best numbers are shown in bold text with blue color for non-learnable methods and red for learnable ones. At the bottom of the table, we report the improvement of AReLU over the best among other non-learnable and learnable methods, in blue and red color respectively.

Learning Rate	$1 \times 10^{-2}$		$1 \times 10^{-3}$		$1 \times 10^{-4}$		$1 \times 10^{-5}$	
Optimizer	Adam	SGD	Adam	SGD	Adam	SGD	Adam	SGD
CELU [2]	98.49	96.56	96.41	75.67	85.62	17.64	34.23	10.79
ELU [7]	98.36	96.64	96.34	65.66	86.77	<b>22.61</b>	28.91	11.36
GELU [13]	<b>98.68</b>	96.02	96.33	14.44	84.45	14.61	20.64	<b>13.30</b>
LeakyReLU [23]	98.29	95.93	96.19	44.76	84.86	13.20	20.55	11.49
Maxout [9]	97.79	96.09	96.45	79.21	85.62	13.99	22.05	10.55
ReLU [26]	98.13	96.33	96.07	49.78	86.07	12.67	19.87	10.24
ReLU6 [18]	98.18	96.05	96.55	56.07	83.42	13.13	17.42	10.27
RReLU [35]	98.52	96.30	95.98	61.78	86.97	10.36	20.61	11.35
SELU [17]	97.72	<b>96.88</b>	<b>97.01</b>	<b>83.85</b>	<b>87.53</b>	22.09	<b>37.98</b>	10.59
Sigmoid	97.62	11.35	85.29	11.35	11.47	11.35	11.35	10.28
Softplus [8]	97.80	93.83	94.58	11.35	75.05	11.35	11.35	10.32
Swish [28]	98.32	95.28	96.47	12.38	85.52	11.82	15.51	10.27
Tanh	97.32	94.40	96.84	69.29	81.50	16.32	29.92	11.35
APL [1] (2)	<b>98.48</b>	96.25	95.50	27.75	80.56	10.28	19.50	15.47
Comb [24] (1)	98.42	96.54	96.07	57.88	85.59	11.67	25.40	10.72
PAU [25] (10)	98.42	<b>97.94</b>	97.07	76.69	89.71	11.35	18.11	14.54
PReLU [11] (1)	98.52	96.10	96.33	61.72	87.24	15.86	18.31	11.40
SLAF [10] (2)	96.69	97.27	95.76	84.13	76.84	15.60	11.19	13.09
AReLU (2)	98.46	97.60	<b>97.29</b>	<b>93.83</b>	<b>90.91</b>	<b>61.06</b>	<b>48.06</b>	<b>19.84</b>
Improvement	-0.22	+0.72	+0.28	+9.98	+3.38	+38.45	+10.08	+6.54
Improvement	-0.02	-0.34	+0.22	+9.70	+1.20	+45.20	+22.66	+4.37



Table 6: Best testing accuracy (%) of five-time training of MNIST-Conv trained for 20 epochs with different learning rates on MNIST. We compare AReLU with 13 non-learnable and 5 learnable activation functions. The number of parameters per activation unit are listed beside the name of the learnable activation functions. The best numbers are shown in bold text with blue color for non-learnable methods and red for learnable ones. At the bottom of the table, we report the improvement of AReLU over the best among other non-learnable and learnable methods, in blue and red respectively.

Learning Rate	$1 \times 10^{-2}$		$1 \times 10^{-3}$		$1 \times 10^{-4}$		$1 \times 10^{-5}$	
Optimizer	Adam	SGD	Adam	SGD	Adam	SGD	Adam	SGD
CELU [2]	98.67	99.05	99.14	97.98	97.88	90.89	91.33	17.39
ELU [7]	98.70	99.04	99.10	97.93	97.96	90.84	91.40	20.51
GELU [13]	99.03	98.99	99.14	97.65	98.04	85.60	90.19	13.30
LeakyReLU [23]	98.79	99.04	99.10	97.85	97.91	90.00	90.90	16.63
Maxout [9]	98.30	98.86	98.82	97.98	97.69	89.98	91.04	23.90
ReLU [26]	98.80	<b>99.06</b>	99.17	97.64	97.85	86.53	89.98	13.95
ReLU6 [18]	98.55	99.01	99.17	98.03	<b>98.14</b>	86.57	88.98	18.79
RReLU [35]	98.98	99.05	<b>99.19</b>	97.90	97.76	88.23	90.31	18.31
SELU [17]	98.53	98.96	98.91	<b>98.04</b>	98.06	<b>92.09</b>	<b>92.26</b>	<b>37.85</b>
Sigmoid	98.99	96.37	98.78	11.35	94.02	11.35	11.35	11.35
Softplus [8]	<b>99.07</b>	98.86	99.04	97.52	96.86	11.88	80.60	16.34
Swish [28]	98.83	98.85	99.09	97.65	97.80	36.30	89.21	10.29
Tanh	97.96	98.89	99.02	97.27	98.09	78.30	88.17	17.76
APL [1] (2)	98.80	99.02	99.00	97.73	97.35	49.37	87.24	16.14
Comb [24] (1)	99.03	99.10	99.16	97.71	97.90	86.52	89.52	12.48
PAU [25] (10)	<b>99.19</b>	99.07	<b>99.18</b>	<b>98.82</b>	98.28	95.75	92.98	15.82
PReLU [11] (1)	98.97	<b>99.11</b>	99.11	97.93	98.07	90.34	91.31	17.82
SLAF [10] (2)	98.88	98.97	98.82	98.50	97.82	94.88	87.67	25.35
AReLU (2)	99.08	99.07	99.05	98.60	<b>98.40</b>	<b>96.32</b>	<b>93.75</b>	<b>85.45</b>
Improvement	+0.01	+0.01	-0.14	+0.56	+0.26	+4.23	+1.49	+47.60
Improvement	-0.11	-0.04	-0.13	-0.22	+0.12	+0.57	+0.77	+60.10



Table 7: Mean testing accuracy (%) of five-time training of MNIST-Conv trained for 20 epochs with different learning rates on MNIST. We compare AReLU with 13 non-learnable and 5 learnable activation functions. The number of parameters per activation unit are listed beside the name of the learnable activation functions. The best numbers are shown in bold text with blue color for non-learnable methods and red for learnable ones. At the bottom of the table, we report the improvement of AReLU over the best among other non-learnable and learnable methods, in blue and red respectively.

Learning Rate	$1 \times 10^{-2}$		$1 \times 10^{-3}$		$1 \times 10^{-4}$		$1 \times 10^{-5}$	
Optimizer	Adam	SGD	Adam	SGD	Adam	SGD	Adam	SGD
CELU [2]	98.62	98.93	99.05	97.73	97.70	89.58	90.58	14.96
ELU [7]	98.55	98.94	99.02	97.82	97.70	89.24	90.46	15.41
GELU [14]	98.85	98.93	<b>99.08</b>	97.51	97.67	51.19	88.94	10.94
LeakyReLU [23]	98.66	98.92	98.96	97.74	97.61	74.01	89.21	13.27
Maxout [9]	98.23	98.78	98.76	97.67	97.46	89.52	90.04	14.85
ReLU [26]	98.72	<b>98.98</b>	99.05	97.57	97.58	81.63	88.88	11.03
ReLU6 [18]	98.51	98.93	99.02	97.79	97.96	81.96	88.14	12.44
RReLU [35]	98.78	98.94	99.06	97.77	97.62	87.64	89.59	13.37
SELU [17]	98.34	98.91	98.84	<b>97.98</b>	97.88	<b>91.56</b>	<b>90.91</b>	<b>33.48</b>
Sigmoid	81.05	96.24	98.72	11.35	92.96	11.35	11.35	10.67
Softplus [8]	<b>98.95</b>	98.78	98.93	97.30	96.57	11.52	78.36	12.50
Swish [28]	98.77	98.80	99.02	97.44	97.51	23.77	88.53	10.05
Tanh	97.91	98.86	98.96	96.94	<b>97.97</b>	75.66	86.99	14.76
APL [1] (2)	98.72	98.92	98.94	97.56	97.22	37.67	84.95	13.52
Comb [24] (1)	98.88	<b>99.01</b>	99.04	97.56	97.55	85.60	88.39	10.94
PAU [25] (10)	<b>99.17</b>	<b>99.01</b>	<b>99.07</b>	<b>98.78</b>	98.15	95.21	92.22	12.86
PReLU [11] (1)	98.89	98.86	99.01	97.81	97.77	88.67	89.69	13.36
SLAF [10] (2)	98.80	98.86	98.67	98.37	97.60	94.61	86.10	18.91
AReLU (2)	98.94	<b>99.01</b>	98.97	98.46	<b>98.22</b>	<b>96.00</b>	<b>93.48</b>	<b>73.00</b>
Improvement	-0.01	+0.03	-0.11	+0.48	+0.25	+4.44	+2.57	+39.52
Improvement	-0.23	+0.00	-0.10	-0.32	+0.07	+0.79	+1.26	+54.09

Table 8: Test accuracy (%) on SVHN by models (with different activation functions) trained directly on SVHN (w/o p.t.), trained on MNIST but not finetuned (w/o f.t.), as well as pretrained on MNIST and finetuned on SVHN (w/ f.t.).

	CELU	ELU	GELU	LReLU	Maxout	RReLU	ReLU	ReLU6	SELU	Sigmoid	Softplus	Swish	Tanh	APL	Comb	PAU	PReLU	SLAF	AReLU
w/o p.t.	15.59	19.59	19.59	19.58	23.01	19.58	19.58	19.96	19.58	19.58	19.58	19.58	19.58	19.58	19.58	19.58	19.58	19.58	<b>24.95</b>
w/o f.t.	28.56	31.95	<b>37.38</b>	28.11	36.52	33.38	36.87	31.74	32.57	15.73	14.39	27.23	21.92	36.20	35.89	24.67	33.45	35.74	31.91
w/ f.t.	71.11	72.39	71.64	72.18	71.88	69.87	70.58	69.90	73.43	33.83	69.18	67.75	64.78	74.21	69.92	74.70	71.15	73.12	<b>76.77</b>



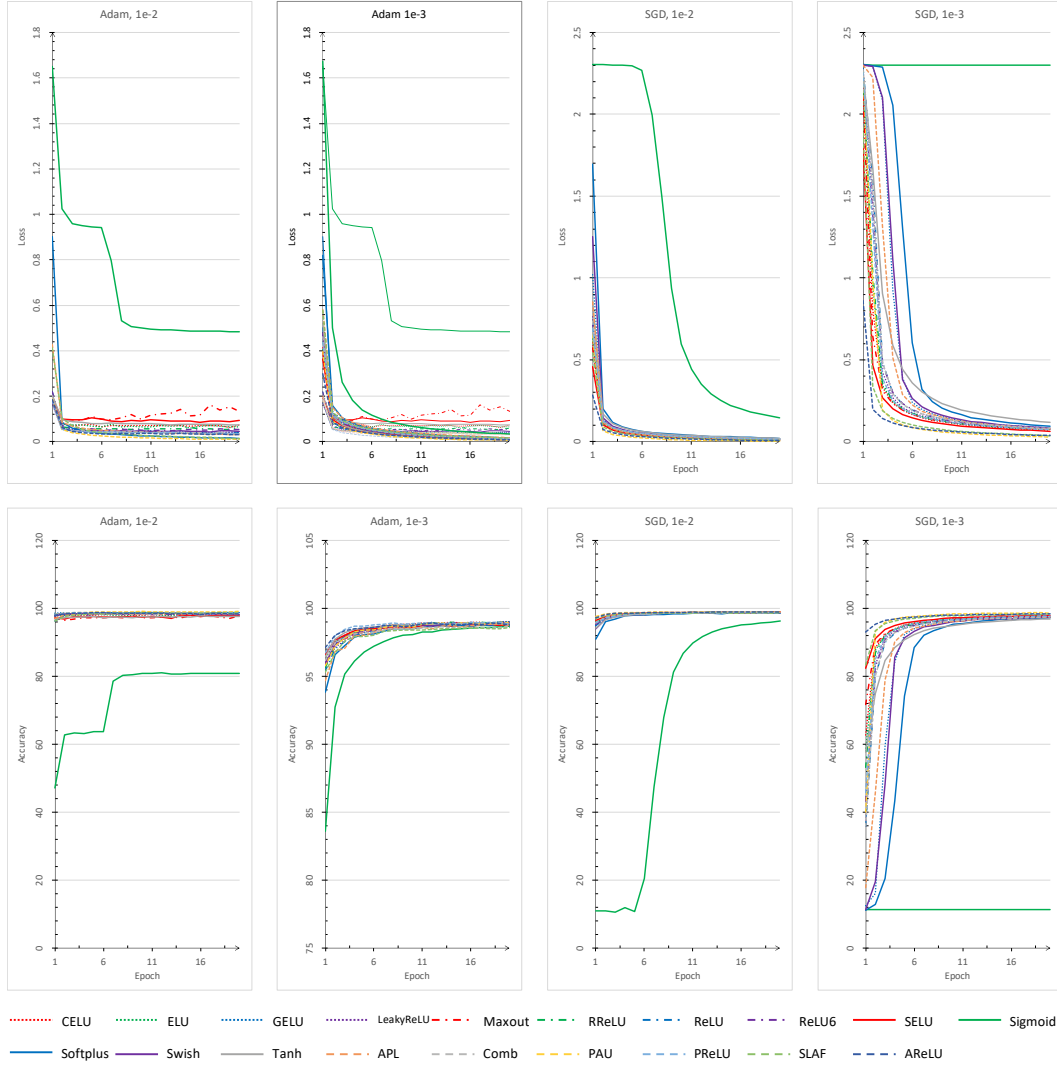


Figure 7: The plots of mean training loss and testing accuracy (%) on MNIST for five-time trainings of MNIST-Conv over increasing training epochs with different optimizers and learning rates.



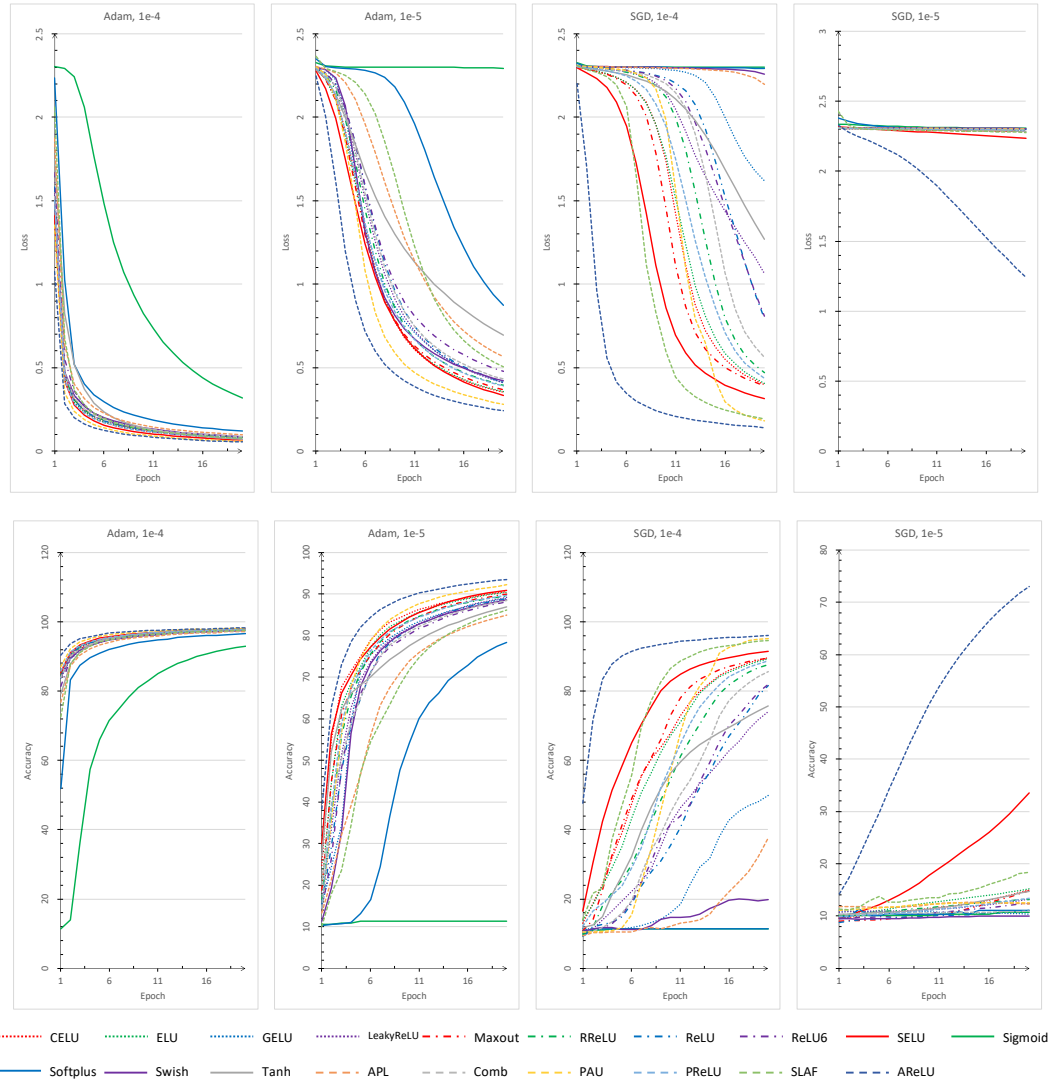


Figure 8: The plots of mean training loss and testing accuracy (%) on MNIST for five-time trainings of MNIST-Conv over increasing training epochs with different optimizers and learning rates.

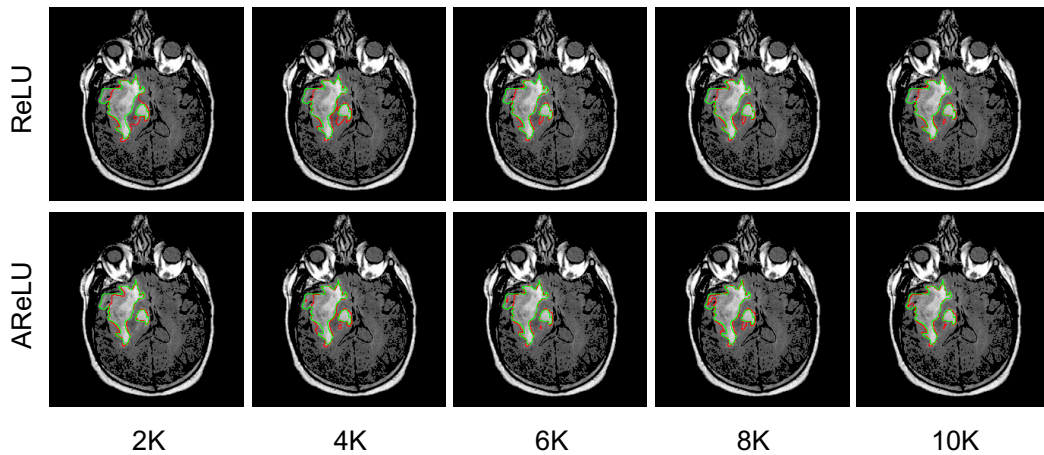


Figure 9: The segmentation results of UNet learned with 2k, 4k, 6k, 8k, 10k iterations.